

Chips of Ti-6Al-2Sn-4Zr-6Mo Alloy – A Detailed Geometry Study

Dmytro Ostroushko, Karel Saksl, Carsten Siemers, Zuzana Rihova

Abstract—Titanium alloys like Ti-6Al-2Sn-4Zr-6Mo (Ti-6246) are widely used in aerospace applications. Component manufacturing, however, is difficult and expensive as their machinability is extremely poor. A thorough understanding of the chip formation process is needed to improve related metal cutting operations. In the current study, orthogonal cutting experiments have been performed and the resulting chips were analyzed by optical microscopy and scanning electron microscopy. Chips from a Ti-6246 ingot were produced at different cutting speeds and cutting depths. During the experiments, depending of the cutting conditions, continuous or segmented chips were formed. Narrow, highly deformed and grain oriented zones, the so-called shear zone, separated individual segments. Different material properties have been measured in the shear zones and the segments.

Keywords—Titanium alloy, Ti-6246, chip formation, machining, shear zone, microstructure

I. INTRODUCTION

TITANIUM alloys are widely used in different branches of industry. Ti-6Al-2Sn-4Zr-6Mo (Ti-6246) is an ($\alpha+\beta$)-alloy showing high strength and excellent corrosion resistance. This alloy is primarily used in rotating components of aircraft engines partly replacing Ti-6Al-4V alloy. Machining of Titanium alloys is complicated due to their high strength. Physical properties like a low heat conductivity results in rapid tool wear. [1]

During machining of Ti-6246 long chips are produced so that cutting operations like turning or drilling need to be interrupted to remove the chips from the process zone. Automation of cutting operations is therefore impossible. [2] The chip formation process needs to be analysed and completely understood to design material and machining conditions and thus improve the machinability. In the present study, orthogonal cutting experiments on a Ti-6246 ingot were performed to investigate the chip formation process. [3]

II. MATERIAL PREPARATION

Chips were produced by orthogonal cutting (see figure 1, left) of a Ti-6246 ingot (figure 1, right). [3] The tool width was larger than the width of cut so that edge effects were minimized.

Ostroushko Dmytro, Slovak Academy of Sciences, Institute of Materials Research, Watsonova 47, 04001 Kosice, Slovakia, email: dimitrij.o@seznam.cz

Saksl Karel, Slovak Academy of Sciences, Institute of Materials Research, Watsonova 47, 04001 Kosice, Slovakia, email: ksaksl@imr.saske.sk
Siemers Carsten, Technische Universität Braunschweig, Institute for Materials, Langer Kamp 8, 38106 Braunschweig, Germany, email: c.siemers@tu-braunschweig.de

Rihova Zuzana, Slovak Academy of Sciences, Institute of Materials Research, Watsonova 47, 04001 Kosice, Slovakia, email: zuzana.rihova@centrum.cz

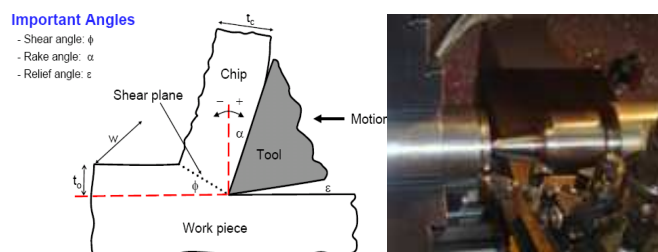


Fig. 1 Left: Visualization of the geometry parameters used in the orthogonal experiments, Right: Experimental set-up of orthogonal cut

In the experiments, seven different cutting speeds v_c (20, 40, 60, 80, 120, 160, 200, 300 m/min) and four cutting depths a_p (0.05, 0.1, 0.15, 0.2 mm) have been chosen. A new standard SECO CNMA 120408 (TK 2000) TiN-coated cutting insert was used for each cut to ensure similar cutting conditions. During the experiments no coolant was used to avoid contaminations.

From the obtained chips a small part (15 to 20 mm) from the beginning of the chip (to minimize tool wear effects) was cut and embedded (polyfast, Isofastat) using 180°C at 3 bars (Buehler – SIMPLIMET 1000). All the specimens were ground with SiC grinding discs (P300, P600, P800, P1200, P2500) and afterwards polished with OP5 suspension (50 ml) having a grain size of 0.06 μm mixed with H_2O_2 (10 ml) on a Buehler PHOENIX 4000 to remove possible surface layers. The etching process was performed with the Kroll solution composed of HF, HNO_3 and H_2O . Cross sections of the chips were afterwards investigated by optical microscope (Olympus GX 71) and scanning electron microscopy observation (Jeol JSM-7000F) and their geometry was measured.

III. RESULTS AND DISCUSSION

The cutting parameters strongly influenced the shape of the chips. Figure 2 shows the three types observed during the experiments, namely, continuous chips showing a constant chips' thickness with high density of zones of localized deformation, see figure 2a, segmented (saw-tooth like) chips in which single segments were separated by shear bands, see figure 2c, and a mixed type of continuous and segmented regions which is the typical appearance of chips being machined at the transition speed, see figure 2b. [4]

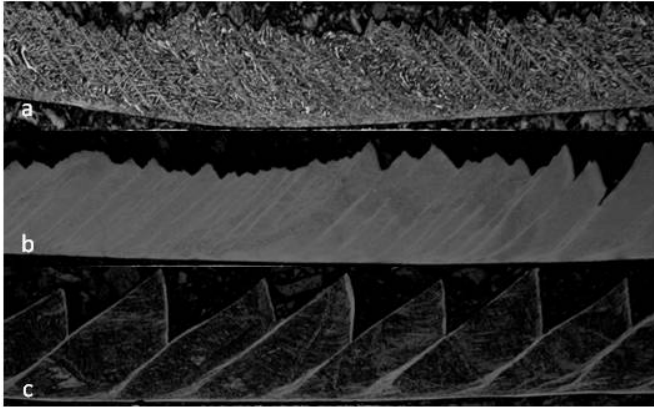


Fig. 2 Optical microscope images of Ti-6246 chips. a: Continuous chips, b: Transition regime, c: Segmented chips

Table I summarizes the optical observations of the chip shapes in dependence of the machining conditions. Continuous chips were only observed at the lowest depth of cuts (0.05 mm and 0.1 mm) and low cutting speeds between 20 m/min and 40 m/min. Transition between continuous and segmented is seen either at the smallest depth of cut (0.05 mm) and medium cutting speeds (80 m/min and 120 m/min) or at the smallest cutting speed (20 m/min) and large depths of cut 0.15 mm and 0.2 mm. Chips made at other conditions were fully segmented.[5]

TABLE I
 DEPENDENCE OF MACHINING CONDITIONS ON SHAPES OF CHIPS,
 CONTINUOUS (C), TRANSITION (T) AND SEGMENTED (S)

Cutting speed v_c [m/min]	Depth of cut a_p [mm]			
	0.05	0.1	0.15	0.2
20	C	C	T	T
40	C	C	S	S
80	T	S	S	S
120	T	S	S	S
160	S	S	S	S
200	S	S	S	S
300	S	S	S	S

Figure 3 shows five main geometrical parameters which were measured from individual chips, namely the maximal and minimal segments' height (h_{max} , h_{min} [mm]), the segments' shear angle (Φ [°]), the segments' width (W [mm]) and the sheared distance (d [mm]).[6]

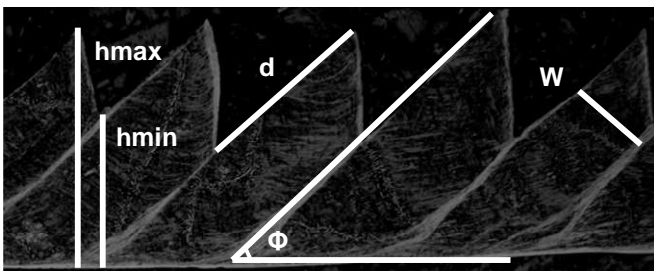


Fig. 3 Geometrical parameters obtained from the chips: Minimum and maximum height h_{max} , h_{min} , shear angle Φ , sheared distance d and segment width W

Figure 4 shows the heights of chips as a function of cutting speed. The black lines represent the maximum height and the red lines indicate the minimum height, respectively. For the depth of cut of 0.05 mm the average maximum height of the chip is larger than 0.05 mm. Assuming volume constancy of the chip its compression ratio is about 140%. Similar results were obtained for a cutting depth of 0.1 mm. In chips with a depth of cut of 0.15 mm, a compression ratio about 140% was observed only for speeds between 40 m/min and 160 m/min. At speeds of 20 m/min and 200 m/min, the average maximum height was similar to the cutting depth. At the maximum cutting speed of 300 m/min the average heights were smaller than the depth of cut by more than 300%. This can be explained by ignition of the chips during the experiments at these extreme cutting conditions. Consequently, at the highest cutting depth (0.2 mm) we finished the experiments at a cutting speed of 200 m/min to avoid machine problems and tool failure.

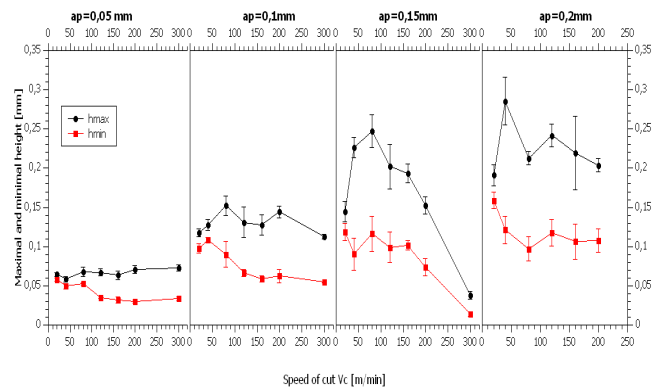


Fig. 4 Chip heights as a function of cutting speed, maximum height (black), minimum height (red)

Figure 5 shows the correlation between the segments' shear angle Φ and the cutting speed for each depth of cut. The red curve represents the measurements performed at the beginning of the chip. The angles indicated by the black curve were measured from the middle of the long chip to study possible influences of tool wear. For the smallest depth of cut we see that the shear angle decreases with cutting speed from approx. 55° to 45°. Shear angles of samples cut at higher cutting depths are around 50° independent of the cutting speed.

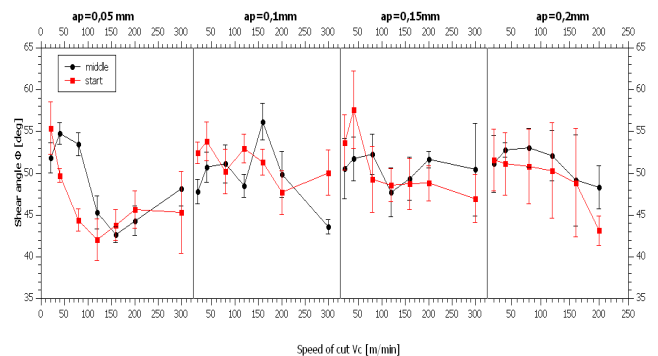


Fig. 5 Correlation between the segments' shear angle Φ and the machining conditions. The red curve represents the begin of cut, the black curve is taken from the middle of the long chips

Figure 6 shows the correlation between the sheared distance d and the cutting speed for each individual depth of cut. The parameter for the first two cutting depths (0.05 mm and 0.1 mm) increases with increasing cutting speed in the range between 80 m/min and 300 m/min. For the chips with cutting depth between 0.15 mm and 0.2 mm, d increases up to 80 m/min and remains almost constant at higher cutting speeds. At 300 m/min d significantly decreases due to chip ignition.

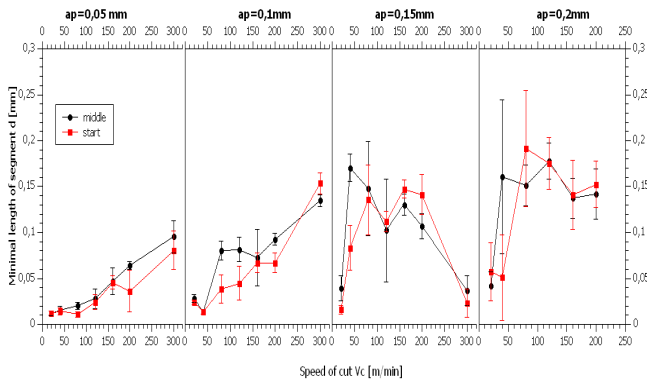


Fig. 6 Correlation between the sheared distance and the cutting speed for different depths of cut, the red curve represents the begin of cut, the black curve is taken from the middle of the long chip

The Width of segments W shows a similar trend as described for the sheared distance. In our analysis we also estimated the widths of the primary shear zones. The average value was calculated from ten regions in the shear zones shown in figure 7. Figure 8 shows the correlation between the shear zone width and the machining conditions. For the first two depths of cut (0.05 mm and 0.1 mm) the average values increase with increasing cutting speed. For chips produced at a depth of cut of 0.15 mm the width of the shear zones increases with increasing cutting speed up to 200 m/min. For a depth of cut of 0.2 mm the parameter substantially increases with increasing cutting speed. In general, the shear zone width increases with increasing cutting depth which can be easily understood by the higher amount of deformation due to the increase in sheared distance.

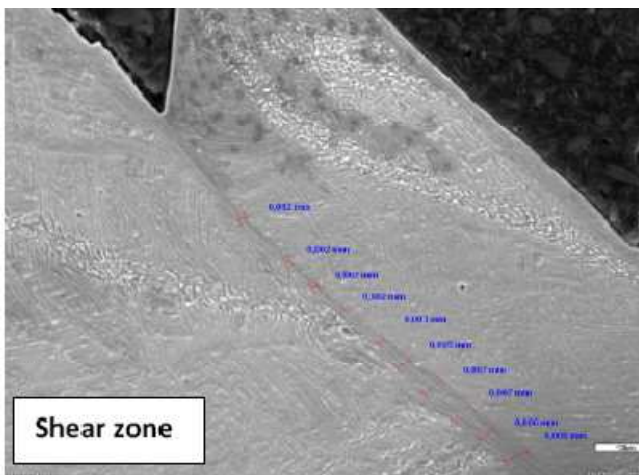


Fig. 7 Shear zone width of a Ti-6246 chip

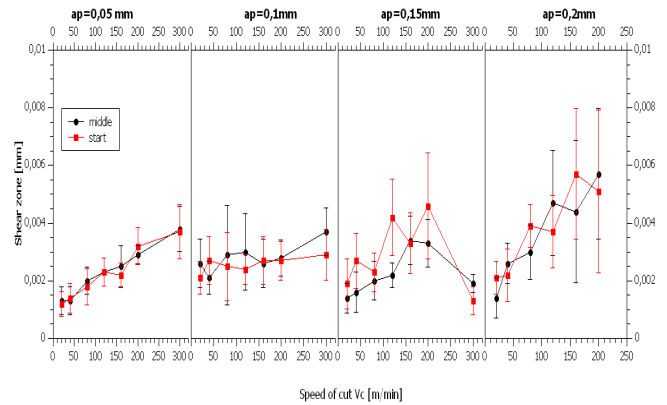


Fig. 8 Correlation between shear zone width and the machining conditions

SEM-EDX

Energy dispersive X-ray Spectroscopy (EDX) analysis on Ti-6246 chips has been performed in order to see possible changes in the phase composition in the material due to the cutting action performed. [7]

Figure 9 shows an SEM image of a continuous chip (a_p : 0.05 mm, v_c : 20 m/min) together with line scan EDX. Based on the analysis we can say that segments and shear zones regions have the same chemical compositions at least within the detection limit of the detector used, see figure 10. A similar conclusion can be drawn for a fully segmented chip (a_p : 0.2 mm, v_c : 200 m/min), see figure 11.

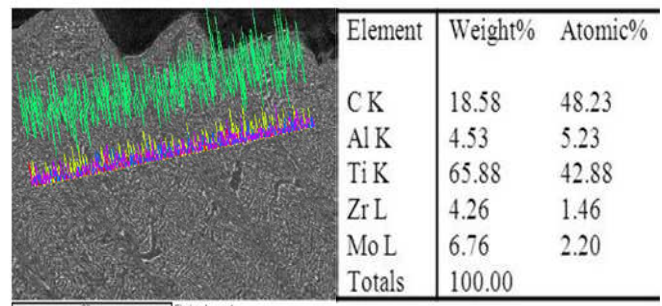


Fig. 9 Linear analyzes of a continuous chip (a_p : 0.05 mm, v_c : 20 m/min). No changes in the local chemistry have been recorded

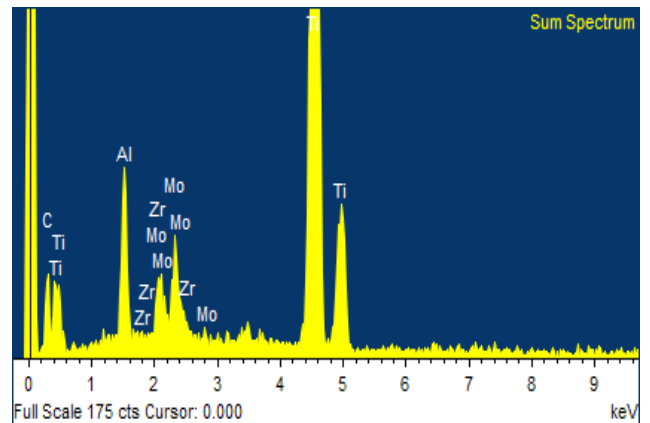


Fig. 10 Cumulated spectrum of the line scans presented in figure 9

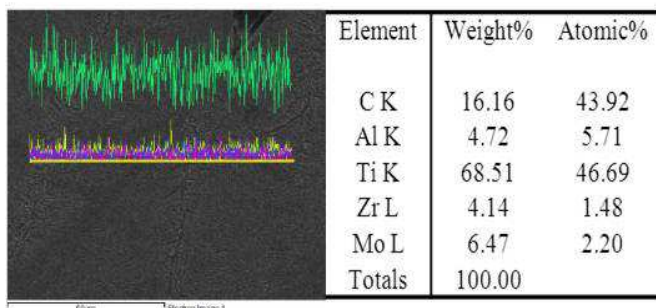


Fig. 11 Linear analyzes of a fully segmented chip (a_p : 0.2 mm, v_c : 200 m/min). No changes in the local chemistry have been recorded

IV. CONCLUSION

In this work, we analyzed geometry of Ti-6246 chips machined in a wide range of cutting conditions, namely a cutting depth between 0.05 mm and 0.2 mm and cutting speeds between 20 mm and 300 m/min. Depending on the machining conditions continuous, segmented or chips with mixed nature formed. In the continuous chips, formed at low depth of cuts (0.05 mm and 0.1 mm) and cutting speed up to 40 m/min, segments are not visible because of the high density of zones of localized deformation. In segmented chips, formed at $a_p = 0.05$ mm above 120 m/min, $a_p = 0.1$ mm above 40 m/min and $a_p = 0.15$ mm and 0.2 mm above 20 m/min, segments are separated by a nanostructured shear zone. Chips showing a mixture of continuous and segmented regions were found at $a_p = 0.05$ mm at cutting speeds between 80 m/min to 120 m/min and at $a_p = 0.15$ mm and 0.2 mm at the lowest speed of 20 m/min.

The geometry of the chips was described by five main geometrical parameters, namely, the maximal and minimal height h_{max} , h_{min} , the segments' shear angle Φ , the segment width W and the sheared distance d . Their dependencies of the machining conditions were shown.

The chemical composition is homogeneous in the chips and corresponds to the chemical composition specified for this alloy. Studies of the chemical composition of the shear zones and its boundaries were performed indicating that the cutting action did not lead to any changes in the local chemistry of Ti-6246 alloy. As the chip formation process is now understood, the machining processes can be improved in a second step.

ACKNOWLEDGMENT

The research leading to these results has received funding from the European Union Seventh Framework Programme (FP7/2007-2013) under grant agreement No. PITN-GA-2008-211536, project MaMiNa. Financial support of the European Commission is therefore gratefully acknowledged.

REFERENCES

- [1] R. Boyer, G. Welsch, E.W. Collins, Materials Properties Handbook: Titanium Alloy, ASM INT. (1994)
- [2] J. Rösler, M. Bäker and C. Siemers, Mechanisms of Chip Formation in H. K. Tönshoff and F. Hollmann (Eds.), Hochgeschwindigkeitsspanen, Wiley-VCH, Weinheim, Germany, (2004).

- [3] C. Leyens and M. Peters, Titanium and Titanium Alloys – Fundamentals and Applications, 2003 WILEY-VCH Verlag GmbH & Co. KGaA, Weinheim, ISBN 3-527-30534-3
- [4] P. Rokicki, Analysis of high-speed machining titanium alloys, SAS Slovakia
- [5] P. Rokicki, K. Nowag, Z. Spetz, L. Fusova, J. Durisin, R. Ghisleni, C. Siemers, Microstructural characteristic of Ti-15V-3Al-3Sn-3Cr chips, Rudy i Metale Niezależne, R.55 / 7 2010, ISSN 0035-9696
- [6] Carsten Siemers, Badya Zahra, Dawid Ksiezzyk, Pawel Rokicki, Zdeněk Spetz, Lenka Fusova, Joachim Rösler, Karel Saks, Chip Formation and Machinability of Nickel-Base Superalloys, Advanced Materials Research (Volume 278) p.460-465 Euro Superalloys 2010.
- [7] J. Goldstein, et al., Scanning Electron Microscopy and X-Ray Microanalysis, Springer, 2003, pp. 271-293